

## A Phosphate Transport System Is Required for Symbiotic Nitrogen Fixation by *Rhizobium meliloti*

Sylvie Bardin, Shan Dan, Magne Osteras,† and Turrough M. Finan\*

Department of Biology, McMaster University, Hamilton, Ontario L8S 4K1, Canada

Received 23 February 1996/Accepted 30 May 1996

**The bacterium *Rhizobium meliloti* forms N<sub>2</sub>-fixing root nodules on alfalfa plants. The *ndvF* locus, located on the 1,700-kb pEXO megaplasmid of *R. meliloti*, is required for nodule invasion and N<sub>2</sub> fixation. Here we report that *ndvF* contains four genes, *phoCDET*, which encode an ABC-type transport system for the uptake of P<sub>i</sub> into the bacteria. The PhoC and PhoD proteins are homologous to the *Escherichia coli* phosphonate transport proteins PhnC and PhnD. The PhoT and PhoE proteins are homologous to each other and to the *E. coli* phosphonate transport protein PhnE. We show that the *R. meliloti* *phoD* and *phoE* genes are induced in response to phosphate starvation and that the *phoC* promoter contains two elements which are similar in sequence to the PHO boxes present in *E. coli* phosphate-regulated promoters. The *R. meliloti* *ndvF* mutants grow poorly at a phosphate concentration of 2 mM, and we hypothesize that their symbiotic phenotype results from their failure to grow during the nodule infection process. Presumably, the PhoCDET transport system is employed by the bacteria in the soil environment, where the concentration of available phosphate is normally 0.1 to 1 μM.**

In the biogeochemical nitrogen cycle, much of the reduction of atmospheric N<sub>2</sub> to ammonia occurs in bacteria within plant root nodules. Molecular genetic studies of bacterial symbiotic mutants have resulted in the identification of nodulation (*nod*) and nitrogen fixation (*nif*) genes whose products are directly involved in the biochemical events which give rise to these nodules. The products of the bacterial *nod* genes synthesize lipooligosaccharide molecules which trigger the dedifferentiation of the plant root cortical cells destined to develop into the nodule primordia (30, 49). Many of the *nif* genes are involved in the regulation or synthesis of the N<sub>2</sub>-fixing enzyme nitrogenase and its accessory proteins (17). The *nod* genes are induced in response to plant flavonoid signals (40), while in planta expression of the nitrogen fixation genes appears to be controlled by oxygen concentration (12, 48).

Mutants which are classified as defective in nodule development (*ndv*) have also been identified. In the alfalfa symbiont *Rhizobium meliloti*, *ndvA*, *ndvB*, *ndvF*, and *exo* mutants form “empty nodules” which contain very few infected cells and fail to fix N<sub>2</sub> (Fix<sup>-</sup>) (15, 19, 29). While the *ndvA* and *ndvB* gene products are involved in production of cyclic β-(1,2)-glucans and *exo* mutants lack a succinoglycan exopolysaccharide, the precise role(s) of these polysaccharides in nodule development remains unclear (14, 28). In *exoD* mutants, the symbiotic phenotype appears to result from an inability of these mutants to grow in planta during the nodule infection process (41).

*R. meliloti* contains two megaplasmids, pSYM and pEXO, which are 1,600 and 1,700 kb, respectively (7, 24, 25, 42). The *nod* and *nif* genes are located on pSYM, and we have previously reported the identification and cloning of the *ndvF* locus, which is located on the pEXO megaplasmid. Here we report

results showing that *ndvF* contains four genes (*phoCDET*) which encode an ABC-type (periplasmic binding protein-dependent) transport system which transports phosphate (P<sub>i</sub>), and likely alkylphosphonates, across the cytoplasmic membrane of *R. meliloti*. We hypothesize that the symbiotic phenotype of the *ndvF* mutants is a direct result of their failure to obtain sufficient phosphorus for growth during the infection process.

### MATERIALS AND METHODS

**Bacterial strains, plasmids, and media.** Bacteria were grown on LB or LBmc medium with antibiotic concentrations as previously described (7). MOPS-minimal medium contained 40 mM morpholinopropanesulfonic acid (MOPS), 20 mM KOH, 20 mM NH<sub>4</sub>Cl, 2 mM MgSO<sub>4</sub>, 100 mM NaCl, 1.2 mM CaCl<sub>2</sub>, and 0.3 μg of biotin per ml. Glucose or succinate was added as a carbon source to a final concentration of 15 mM. *R. meliloti* Rm 1021 is a streptomycin-resistant derivative of SU47. Strain Rm G439 is a strain Rm 1021 derivative in which the 12-kb *Hind*III fragment containing the *ndvF* locus was replaced with the internal neomycin resistance (Nm<sup>r</sup>) *Hind*III fragment of Tn5; *R. meliloti* Rm G490 (*phoC490*) and Rm G491 (*phoT491*) are strain Rm 1021 derivatives in which an ΩSp<sup>r</sup> interposon was inserted in the first and third *Eco*RI sites within *ndvF*, respectively (8). pTH38 contains the complete *ndvF* locus cloned in a 7.3-kb *Bam*HI fragment in pRK7813, and pTH21 is a pLAFR1 cosmid clone carrying the complete *ndvF* locus within a 22-kb region (8).

**Genetic techniques, DNA manipulations, and sequencing.** Bacterial matings were performed as previously described (7). Tn5-B20 (45) insertions in *ndvF* were identified following mutagenesis of pTH21 by using *Escherichia coli* MT607::Tn5-B20 as transposon donor. Tn5-B20 insertions in the plasmid DNA were determined by restriction and DNA sequence analysis. Standard methods were used for plasmid DNA isolation, restriction digestion, agarose and polyacrylamide gel electrophoresis, ligations, and transformation (44).

Plasmids pTH38 and pTH38ΩB8::Tn5 were used as the sources of material for DNA sequencing (Fig. 1). Restriction fragments were subcloned into pUC118 and pUC119 and used for construction of unidirectional nested deletions by exonuclease III treatment followed by S1 nuclease digestion (21). The nucleotide sequence was determined from single-stranded DNA obtained from host strain XL-1Blue (Stratagene) following infection with helper phage M13K07 (52). DNA sequencing was performed by dideoxy chain termination according to the protocol of United States Biochemicals for the Sequenase 2.0 enzyme, by using [α-<sup>35</sup>S]ATP (NEN/DuPont) and 7-deaza dGTP (Pharmacia). Both strands of DNA were sequenced. TnphoA insertion sites in pTH38 were sequenced directly from double-stranded DNA by using the *phoA*-specific primer (5'-AATATCGC CCTGAGC-3'). Tn5-B20 insertion sites were sequenced by using the universal -20 (*lacZ*) primer (5'-GTAACACGACGCGCCAGT-3'). 7A, 19, 4B, and 17 had inserted at nucleotide positions 1792, 2862, 4481, and 5211, respectively (Fig. 1).

\* Corresponding author. Mailing address: Dept. of Biology, McMaster University, 1280 Main St. West, Hamilton, Ontario L8S 4K1, Canada. Phone: (905) 525-9140, ext. 22932. Fax: (905) 522-6066. Electronic mail address: FINAN@MCMASTER.CA

† Present address: Laboratoire de Biologie, Végétale et Microbiologie, URA CNRS 1114, Université de Nice Sophia-Antipolis, Parc Valrose, 06108 Nice Cedex 02, France.

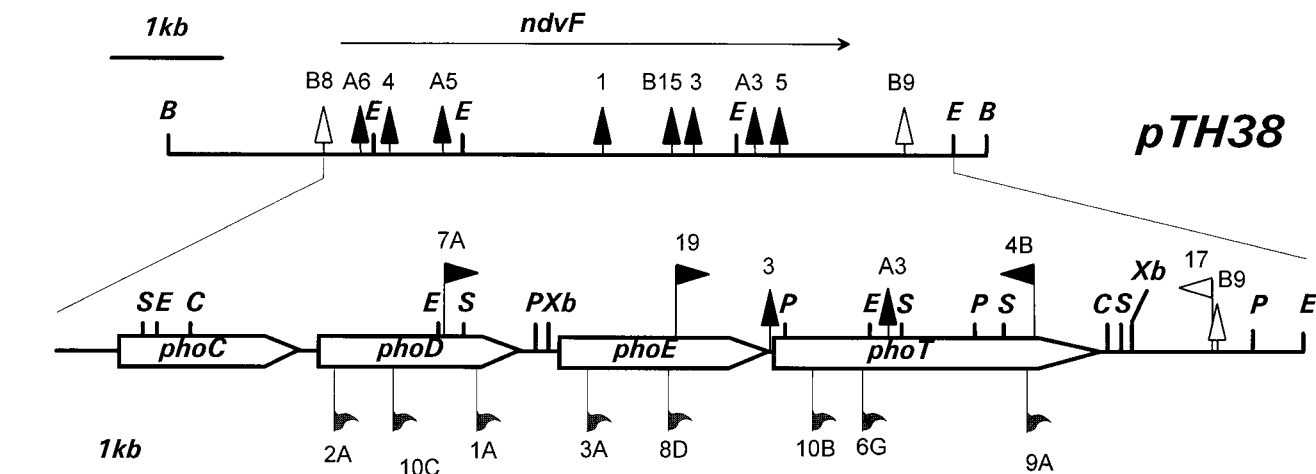


FIG. 1. (Top) Physical and genetic map of the *ndvF* locus of *R. meliloti* cloned in pTH38. The horizontal arrow above the pTH38 map shows the direction of transcription of *ndvF* as previously determined from the orientation of Tn<sub>5</sub>*phoA* fusions. Filled (Fix<sup>-</sup>) and open (Fix<sup>+</sup>) arrows indicate locations of Tn5 insertions that do and do not, respectively, abolish the ability of pTH38 to complement the Fix<sup>-</sup> phenotype of the *ndvF* deletion mutant RmF114 (8). (Bottom) The sequenced region (from insertion B8 to the indicated *EcoRI* site). The four ORFs, *phoC*, *phoD*, *phoE*, and *phoT*, are indicated. Also indicated are the locations of four Tn5-B20 insertions (flags facing up) and eight Tn<sub>5</sub>*phoA* fusions (flags facing down). The direction of the flag points indicates the orientation of the *lacZ* and *phoA* genes. Restriction sites shown are *Bam*HI (B), *Cl*aI (C), *Eco*RI (E), *Pst*I (P), *Sal*I (S), and *Xba*I (Xb).

DNA and derived protein sequences were analyzed with the PC/Gene (Intelligenetics), Blast (2), CLUSTALV (23), and Top Pred II (10) software packages.

**RNA extraction and primer extension.** RNA was extracted from wild-type *R. meliloti* 1021 cultures as previously described (39). The purity and quality of the RNA were checked by electrophoresis through a 1.2% agarose gel with Tris-acetate-EDTA (TAE) running buffer. The contaminating DNA was removed by treatment with 270 U of RNase-free DNase (Boehringer-Mannheim) per ml for 30 min at 37°C in the presence of 6 U of RNase inhibitor (RNAguard; Pharmacia) per ml. This was followed by a phenol-chloroform-isoamyl alcohol (25:24:1) extraction and ethanol precipitation of the RNA.

To identify the transcription start site of the *phoC* mRNA, a specific oligonucleotide (5'GTCTTCTTGCCGAAGTGGCGGGTTACGTTTC3') complementary to the beginning of the coding region of the gene was synthesized (Mobix; McMaster University). End labelling and extension of the primer with avian myeloblastosis virus reverse transcriptase were performed as previously described (39).

**Transport and growth experiments.** For phosphate transport assays, LBmc-grown cells were washed twice with MOPS-minimal medium, subcultured (1:50 dilution) into phosphate-free MOPS-minimal medium, and incubated with shaking (200 rpm) overnight at 30°C. Cells were harvested by centrifugation, washed at 4°C in MOPS minimal medium (without P [-P]), resuspended in the same medium to an optical density at 600 nm of 5, and stored at 4°C. For phosphate uptake assays, the cells were diluted 1:20 into MOPS minimal medium (-P) and incubated at 30°C for 5 min. A 12- $\mu$ l volume of <sup>33</sup>P<sub>i</sub> (60  $\mu$ Ci/ $\mu$ mol) was added to a final concentration of 10  $\mu$ M. Aliquots (100  $\mu$ l), removed at various times, were placed on a 0.45- $\mu$ m-pore-size nitrocellulose filter (presoaked in 1 M K<sub>2</sub>HPO<sub>4</sub>) and immediately washed with MOPS minimal medium (-P). Filters were dried, placed in liquid scintillation vials with scintillation fluid, and counted in a scintillation spectrophotometer. For all experiments, we used chloroform-treated cells to determine the amount of background binding of <sup>33</sup>P<sub>i</sub> to the bacterial cells. Succinate uptake experiments employing [<sup>14</sup>C]succinate (2.5  $\mu$ Ci/ $\mu$ mol) at a final concentration of 40  $\mu$ M were done as previously described (56).

To test strains for P utilization ability, cultures grown in LBmc were diluted 1:1,000 into 5 ml of MOPS-buffered minimal medium containing the indicated phosphorus sources at 2 mM. Cultures were grown with shaking at 30°C, and growth was monitored by measuring the optical density at 600 nm.

$\beta$ -Galactosidase and alkaline phosphatase (AP) assays were performed with aliquots of cells from 5-ml cultures as previously described (39, 56).

**Nucleotide sequence accession number.** The nucleotide sequence (5,705 bp) of the *ndvF* locus of *R. meliloti* has been deposited in GenBank under accession number U59229.

## RESULTS

**Nucleotide sequence of the *ndvF* locus.** The *ndvF* locus was previously localized to a 7.3-kb *Bam*HI fragment cloned in plasmid pTH38. Transposon Tn5 insertion mutagenesis of pTH38 followed by complementation analysis further localized

*ndvF* to a 5-kb region between the Fix<sup>+</sup> insertions B8 and B9 (Fig. 1). We have determined the nucleotide sequence for both strands of the 5,705-bp region from insertion B8 to the *Eco*RI site located 493 nucleotides beyond insertion B9 (Fig. 1). Analysis of this sequence revealed four nonoverlapping open reading frames (ORFs) encoding proteins of 270, 300, 320, and 505 amino acids, which we designated PhoC, PhoD, PhoE, and PhoT, respectively (Fig. 1). The four genes are transcribed in the direction predicted in a previous study employing AP gene fusions to the *ndvF* locus (8). A clear G+C bias was observed at the third nucleotide position of the codons within each ORF (79 to 83%), relative to the general G+C content (64%), and the results (not shown) of a codon preference plot employing an *R. meliloti* codon usage table suggested that the four predicted genes were expressed in *R. meliloti* (20). Putative ribosome-binding sites were identified for all ORFs, between 5 and 9 bp upstream of the ATG start codons (AGGAAN<sub>9</sub>ATG, GAGAAN<sub>8</sub>ATG, CGGAAN<sub>5</sub>ATG, and TAGGAN<sub>7</sub>ATG, respectively). The intergenic regions were 117 bp long between *phoC* and *phoD*, 172 bp long between *phoD* and *phoE*, and 9 bp between *phoE* and *phoT*. While it appears likely that these four genes compose an operon, further experiments are required to conclusively establish this supposition.

**Characterization of the encoded proteins.** A BLASTX search of GenBank revealed that the *ndvF*-encoded proteins were similar to the *E. coli* *phnC*, *phnD*, and *phnE* gene products (2, 9). The PhoC and PhoD proteins were homologous to PhnC and PhnD, respectively, while the PhoT and PhoE proteins were homologous to each other and to the *E. coli* PhnE protein. The *E. coli* *phn* genes are required for the transport and catabolism of phosphonates and are transcribed as an 11-kb operon (54). Phosphonates are organophosphorus compounds which have direct C-P bonds rather than the common C-O-P phosphodiester linkage. Sequence analysis and experimental evidence suggest that the *E. coli* *phnC*, *phnD*, and *phnE* genes encode a phosphonate and phosphate transport system of the ABC (ATP-binding cassette) class (54). In gram-negative bacteria, these transport systems are made up of a periplasmic binding protein, one or two integral membrane proteins, and a hydrophilic ATP-binding protein (13, 22).

CLUSTALV alignments of the *R. meliloti* Pho and *E. coli* Phn proteins are shown in Fig. 2. The PhoC and PhnC proteins are 43% identical. They are homologous to the highly conserved ATPase component of the ABC transport systems and contain the two Walker motifs associated with many nucleotide-binding proteins (residues 34 to 42 and 165 to 170) (Fig. 2; boxes A and B). The amino terminus of the PhoD protein has characteristics of an export signal sequence, such as a basic amino terminus, a hydrophobic core, and in this case two cleavage sites (amino acids 19/20 and 21/22) which conform to the (-3, -1) rule (37). This is in agreement with the periplasmic location of the substrate-binding protein present in all ABC transporters that mediate solute uptake (22). The *R. meliloti* PhoT protein contains 505 amino acid residues, and while it is much larger than the *R. meliloti* PhoE (320 amino acids) and *E. coli* PhnE (276 amino acids) proteins, its C-terminal 200 amino acids have a high level of homology with those two proteins (Fig. 2). This size difference is reminiscent of that found between the analogous integral membrane proteins MalF (514 amino acids) and MalG (296 amino acids) of the ABC-type maltose transport system of *E. coli* (11, 18).

**Membrane topology of the PhoCDET proteins.** In a previous study, we isolated mutants with *ndvF::TnphoA* gene fusions which expressed AP activity (8). Such fusions are generally only active when AP is fused to an exported protein or to the external domain of a transmembrane protein (35). Analysis of the DNA sequence of the *ndvF::TnphoA* fusion junctions (Fig. 1) revealed that all formed in-frame protein fusions between AP and the predicted PhoD, PhoE, and PhoT proteins. No *TnphoA* insertions which expressed AP activity were located in the *phoC* gene. This is not surprising in view of the similarity between PhoC and the hydrophilic ATP-binding component of ABC transport systems; these proteins appear to be located in the cytoplasm, where they associate with the cytoplasmic membrane (22; see also reference 3). The three *ndvF::TnphoA* insertions (2A, 10C and 1A, Fig. 1) which showed the highest level of AP activity were located in the *phoD* gene. Together with the predicted N-terminal secretory leader peptide of PhoD, these data are consistent with the proposed role of PhoD as a periplasmic binding protein.

Of the remaining five *TnphoA* insertions, 3A and 8D fused AP to PhoE at amino acid residues 51 and 188, respectively, while 10B, 6G, and 9A fused AP to PhoT at amino acid residues 62, 239, and 397, respectively. Hydrophobicity plots of PhoE and PhoT revealed that each of these proteins contains four "certain" and two "putative" transmembrane domains (Fig. 2) (10). Consistent with the positive-inside rule (53), if we assume that there are six transmembrane domains and that the N termini are in the cytoplasm, we calculate a lysine-plus-arginine cytoplasmic-domain bias of 10 for PhoE and 8 for PhoT. AP fusion 3A in PhoE and fusions 10B and 6G in PhoT are located between the first and second predicted transmembrane domains (boxes 1 and 2 in Fig. 2). Therefore, for these fusions to be external, the N termini of the PhoE and PhoT proteins must be located in the cytoplasm. When this topology is extended across the protein, we note that insertion 9A in PhoT is located in the second predicted periplasmic domain (between boxes 3 and 4 in Fig. 2). Insertion 8D fuses AP to PhoE, 4 amino acids from the C-terminal end of the predicted third transmembrane domain; we assume that this fusion extends into the periplasm. In comparing the derived topologies of PhoE and PhoT, it is evident that much of the difference between these two proteins resides in the 258-amino-acid periplasmic loop of PhoT, which is very large in comparison with the equivalent 76-amino-acid loop of PhoE (see regions between boxes 1 and 2 in Fig. 2).

#### Phosphate and phosphonate phenotype of *ndvF* mutants.

The above results prompted us to examine the ability of wild-type *R. meliloti* and three *ndvF* mutants to utilize various sources of phosphorus for growth in MOPS-buffered minimal medium. We compared the parental strain 1021 with the insertion mutants Rm G490 (*phoC490*) and Rm G491 (*phoT491*) and the deletion strain Rm G439, in which a 12-kb region including the *phoCDET* genes has been removed. Whereas the wild type and mutants grew well in media containing 2 mM glycerol-3-phosphate or aminoethylphosphonate as P sources, all three mutants grew very poorly in media containing 2 mM  $P_i$  as the P source (Fig. 3; data for *R. meliloti* Rm 490 and Rm 491 were similar). These results suggested that the mutant strains were defective in  $P_i$  assimilation.

The deletion strain, Rm G439, grew poorly with aminomethyl- or methylphosphonate as the P source, while growth of the *phoC* and *phoT* insertion mutants, Rm G490 and Rm G491, on these phosphonates was similar to that of the wild type (Fig. 3 and data not shown). Limited DNA sequencing of regions outside the *phoCDET* genes, but within the region deleted in strain Rm G439, has revealed a gene homologous to the *phnM* gene of *E. coli* (9); the *phnM* gene product is believed to be part of an enzyme complex (C-P lyase) which cleaves the C-P bond upon entry of the phosphonate into the cell. We assume that deletion of *phnM* (and perhaps other *phn* genes) in strain Rm G439 inactivates the C-P lyase with the result that Rm G439 cannot degrade or grow in media containing aminomethyl- and methylphosphonate as P sources. The growth of the *phoC* and *phoT* mutants with aminomethyl- and methylphosphonate suggests that these compounds can be transported by an alternate system in *R. meliloti*. It is not yet clear whether the PhoCDET proteins are involved in phosphonate uptake. In this respect, we note that *Enterobacter aerogenes* has two phosphonate degradative pathways (27).

To determine the nature of the phosphate utilization defect in the *ndvF* mutants, we examined phosphate-starved cells of the wild type and the *ndvF* mutant Rm G439 for their ability to take up  $^{33}P_i$ . As a positive control, we examined the ability of the same cells to transport [ $^{14}C$ ]succinate (Fig. 4). Unlike the parent strain Rm 1021, the *ndvF* mutant failed to transport phosphate, whereas both strains transported succinate at similar rates. Together, the uptake, growth, and sequence homology data show that the *ndvF* locus encodes an uptake system which transports  $P_i$ , and possibly phosphonates, across the cytoplasmic membrane.

**Phosphate control of *ndvF* expression.** To determine whether expression of the *ndvF* locus responds to available phosphate, we employed Tn5-B20 (45) to generate transcriptional gene fusions between *lacZ* and *ndvF* on the cosmid pTH21. The DNA sequences of the fusion junctions of four Tn5-B20 insertions which lay within the 7.3-kb *Bam*HI restriction fragment were determined (Fig. 1). Insertions 7A and 19 were located in, and transcribed in the same direction as, the *phoD* and *phoE* genes, respectively. Insertion 4B was in the *phoT* gene, and the direction of transcription of *lacZ* was opposite to that of *phoT*. Insert 17 lay downstream of the *phoCDET* genes. Employing these plasmid-borne gene fusions in an *R. meliloti* Lac<sup>-</sup> background, we assayed for  $\beta$ -galactosidase activities in cells cultured in a MOPS-buffered minimal medium with added phosphate (2 mM) and without added phosphate (Fig. 5). We also measured AP activity, as this activity is known to be derepressed in P-limited cultures (46, 54). As expected, we observed high-level AP activities in all cells cultured in the absence of added P and low-level activity in cells grown in the media containing P (Fig. 5, open bars). The  $\beta$ -galactosidase activities of strains carrying insertion 4B



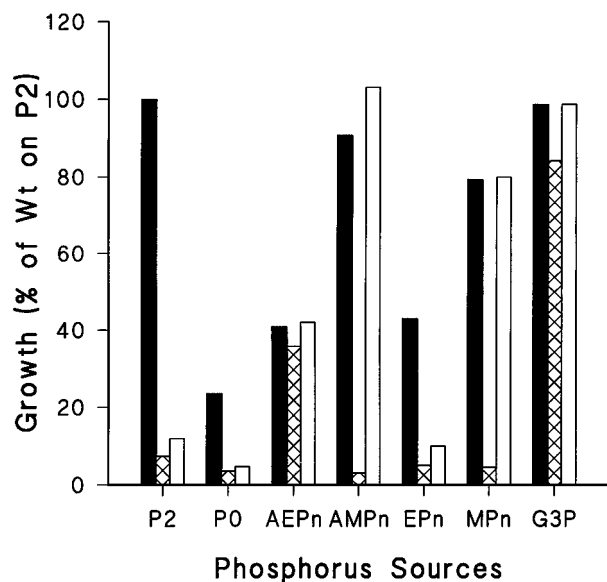


FIG. 3. Histogram representing the growth of wild-type *R. meliloti* Rm 1021 (black bars), the *phoCDET* deletion mutant, Rm G439 (cross-hatched bars), and the *phoC490* insertion mutant, Rm G490 (open bars), when supplied with various sources of P. MOPS-minimal medium contained no phosphate (P0), 2 mM  $P_i$  (P2), 2 mM aminoethylphosphonate (AEPn), 2 mM aminomethylphosphonate (AMPn), 2 mM methylphosphonate (MPn), 2 mM ethylphosphonate (EPn), or 2 mM glycerol-3-phosphate (G3P). The optical density at 600 nm ( $OD_{600}$ ) measured after 60 h is reported as a percentage of the growth of strain 1021 in 2 mM  $P_i$  ( $OD_{600} = 0.8$ ). Values are the means of triplicate determinations.

or 17 were similar under the two growth regimes; however, the *phoD* and *phoE* gene fusions 19 and 7A were induced 10- to 25-fold in response to phosphate starvation (Fig. 5, black bars). Thus, expression of *phoD* and *phoE* is depressed in response to limiting phosphate. The substantially lower level of  $\beta$ -galactosidase activity detected from the strain with the *phoE* gene fusion (fusion 19) in comparison with that for the *phoD* fusion (fusion 7A) suggests that these genes may be differentially expressed. In agreement with this suggestion, we note that an examination of the previously reported AP activities derived from strains carrying the *pho::TnphoA* insertions (Fig. 1) reveals that the levels of activity from strains with the *phoD* insertions (2A, 10C, and 1A) were at least three times higher than the activity from *phoE* or *phoT* insertion strains (3A, 8D, 10B, 6G, and 9A) (see Fig. 2 in reference 8). It is possible that the 172-bp *phoD-phoE* intergenic region has a role in regulating *phoE* and *phoT* expression.

To map the transcription start site of *phoC*, we extracted mRNA from cells grown in LBmc, as we have observed that the expression level of the *phoD* and *phoE lacZ* fusions (fusions 7A and 19) was high in LBmc-grown cells. In two separate experiments, we extended a primer from the 5' end of *phoC* (see Materials and Methods) and observed one major transcript which started 40 bp upstream of the translational start codon (Fig. 6). Analysis of this region revealed a possible -10 region preceded by two tandem 18-bp sequences, located at bp -23 to -40 and -45 to -62 relative to the transcriptional start site, which share 12 and 11 identical nucleotides, respectively, with the PHO box consensus CTGTCATA(A,T)A(A,T)CTGTCA(C,T) of *E. coli* (33, 54).

## DISCUSSION

The data in this paper demonstrate that the *ndvF* locus of *R. meliloti* consists of four genes, *phoCDET*, which together code

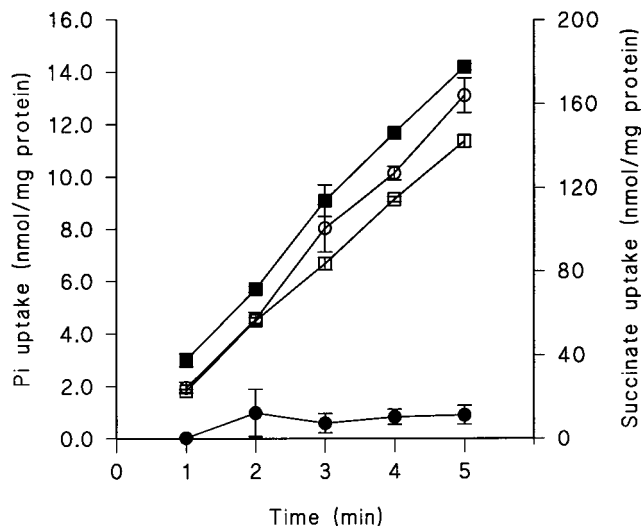


FIG. 4. Uptake of phosphate and succinate by phosphate-starved cells of strains Rm 1021 (■, □) and Rm G439 (●, ○). Closed symbols indicate phosphate uptake, and open symbols indicate succinate uptake. The cells were starved for 24 h in a phosphate-free MOPS medium containing 15 mM succinate and 15 mM glucose as carbon sources. The uptake experiment was performed in the same medium except that glucose was provided as an energy source.  $10 \mu\text{M } ^{32}\text{P}_i$  and  $40 \mu\text{M } [^{14}\text{C}]\text{succinate}$  were added to the medium for the phosphate and succinate uptake assays, respectively. Values are the means of triplicate determinations  $\pm$  standard errors.

for an ABC-type solute uptake system that transports phosphate, and possibly phosphonates, across the cytoplasmic membrane. *R. meliloti ndvF* mutants form root nodules which fail to fix  $\text{N}_2$  ( $\text{Fix}^-$ ). In many of these mutant nodules, the infection process is blocked early, before release of the bacteria from the infection threads (8). Given that we now know that the *ndvF* locus encodes a phosphate transport system, and that *ndvF* mutants fail to grow in defined medium containing 2 mM  $\text{H}_2\text{PO}_4^-$  as the sole P source, it seems likely that the  $\text{Fix}^-$  symbiotic phenotype results from an inability of the mutants to

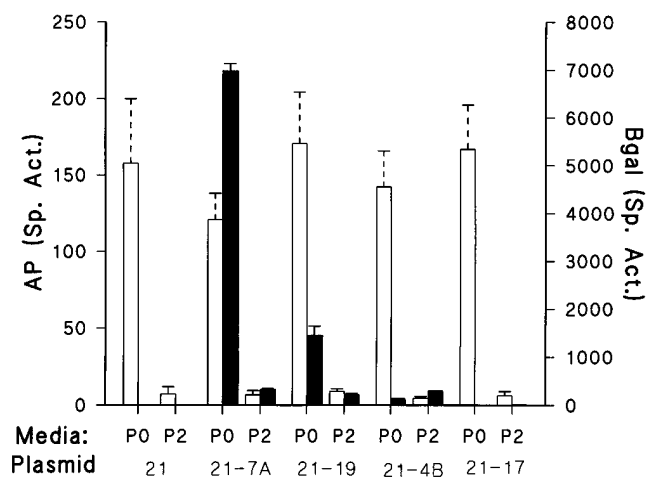


FIG. 5. Effect of phosphate on expression of *phoD::lacZ* and *phoE::lacZ* gene fusions. *R. meliloti* cells carrying Tn5-B20 insertions in plasmid pTH21 were cultured in MOPS-minimal medium containing no added  $P_i$  (P0) or 2 mM  $P_i$  (P2). Specific activities (Sp. Act.) for  $\beta$ -galactosidase (Bgal) (closed bars) and AP (open bars) were determined. Values are the means  $\pm$  standard errors of the mean for triplicate assays.

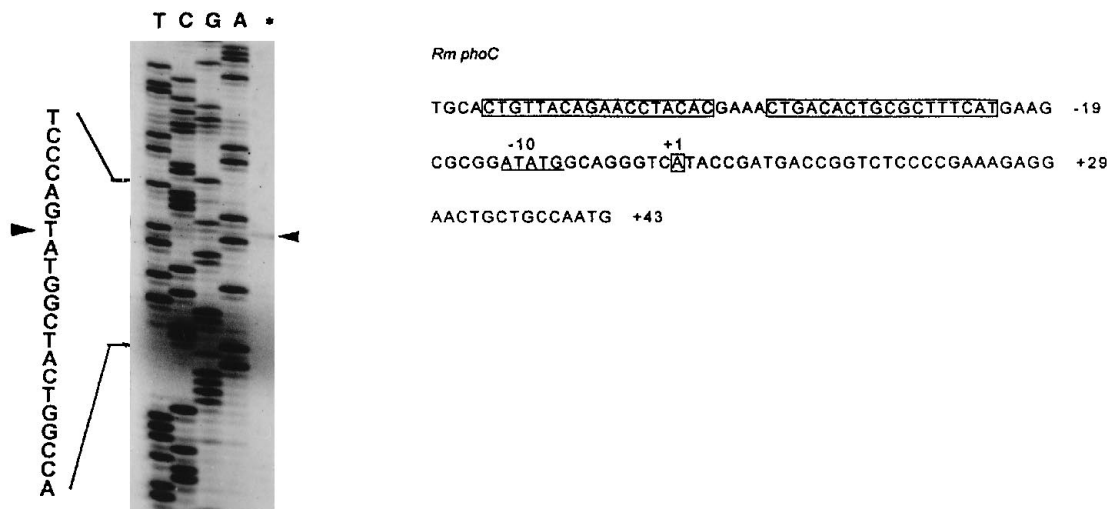


FIG. 6. Promoter analysis of *R. meliloti* (*Rm*) *phoC* gene. The autoradiograph contact print shows the primer extension product (lane \*) (30  $\mu$ g of RNA from LBmc-grown strain Rm 1021) and the products of sequencing reactions with the same primer. The relevant sequence is shown on the left of the gel, and the position of the extension product is indicated by an arrowhead. On the right is shown the promoter region of *R. meliloti phoC*. The transcription start site is indicated by +1, the -10 region is underlined, and the boxed sequences indicate the positions of the two putative PHO boxes.

grow during the infection process within the nodule. The *ndvF* mutants exhibit a delay in inducing root nodules in comparison with nodule development with the wild-type strain (8). This delay may also result from reduced bacterial growth, and thus requirement for a longer time period to reach a cell density such that sufficient Nod factor signal is synthesized to trigger root nodule formation (30). There are other possible explanations for the symbiotic phenotype of the *ndvF* mutants; for example, the P status of the bacteria may be involved in the regulation of other cellular processes involved in the symbiosis. In this respect, it is interesting that in the plant pathogen *Agrobacterium tumefaciens*, phosphate starvation increases the expression of the central virulence regulatory gene, *virG* (55). We are currently investigating the nature of the symbiotic defect by characterizing strains carrying second-site mutations which suppress the  $\text{Fix}^-$  phenotype of the *ndvF* mutants (38). The elucidation of the biochemical mechanism of suppression will clarify the role of the *ndvF* locus in nodule development.

The conclusion that the *phoCDET* genes encode a periplasmic binding protein-dependent system for the transport of phosphate and likely phosphonates is based on (i) the high degree of homology of PhoC to the ATP-binding proteins of the ABC-type transport systems and the deduced topology of the PhoD, PhoE, and PhoT proteins; (ii) the fact that *phoCDET* mutants fail to grow in defined media containing 2 mM  $\text{P}_i$ ; and (iii) the failure of the *phoCDET* deletion mutant, RmG439, to transport  $^{33}\text{P}$ -labelled phosphate despite its ability to transport succinate at wild-type rates.

The inability of the *R. meliloti phoCDET* mutants to grow when P is supplied as 2 mM  $\text{P}_i$  suggests that the *phoCDET* genes encode the sole phosphate transport system in *R. meliloti*. Conversely, the growth of the *phoCDET* insertion and deletion mutants in media containing 2 mM glycerol-3-phosphate or aminoethylphosphonate indicates that there are separate uptake systems for these compounds in *R. meliloti*. The existence of distinct phosphate and glycerol-3-phosphate uptake systems in many bacterial species is well-known (e.g., see reference 26), and *E. aerogenes* probably has two separate phosphonate transporters capable of aminoethylphosphonate transport (27). Data from uptake experiments employing cells

of various *Rhizobium* species grown under P-limiting and P-excess conditions also led other workers to conclude that rhizobia contain a single, repressible, energy-dependent phosphate transport system (47). However, bacterial phosphate transport is best characterized in *E. coli* and *Acinetobacter johnsonii*, and both of these organisms contain two major  $\text{P}_i$  transport systems: one is a low-affinity system (*pit*) which is believed to be constitutively expressed, and the other is a high-affinity, binding protein-dependent system (*pstSCAB*) which is expressed under phosphate-limiting conditions (43, 50, 51). We believe that it is premature to conclude that *R. meliloti* contains a single phosphate transport system, as we recently identified a *pit*-like gene, and the expression and regulation of this gene are currently under investigation (4). The PhoCDET proteins of *R. meliloti* are clearly similar to the phosphonate uptake proteins PhnCDE of *E. coli* (Fig. 2) rather than to the proteins of the *pstSCAB*-encoded high-affinity phosphate transport system of *E. coli*. The phosphonate transport genes are cryptic in *E. coli* K-12-derived strains (34); however, when this system is active, there is good evidence that it can transport  $\text{P}_i$  in addition to phosphonates (36). Further experiments are required to definitively establish that the *R. meliloti* PhoCDET system also transports phosphonates. In this respect, we note that in one study, all of the members of the family *Rhizobiaceae* examined were able to utilize methyl-, ethyl-, aminomethyl-, and aminoethylphosphonate as sole sources of P (32).

In view of the very low concentrations of soluble  $\text{P}_i$  in most soils (0.1 to 10  $\mu\text{M}$ ) (6), it is possible that the acquisition of phosphate plays an important role in the growth and survival of soil microorganisms. In this respect, it is interesting that Beck and Munns (5) found a large variation in the ability of strains from various *Rhizobium* species to grow and survive at very low phosphate concentrations. Moreover, Almendras and Bottomley (1) and Leung and Bottomley (31) have presented strong evidence to establish a link between the phosphate-sequestering abilities of *Rhizobium trifolii* strains and nodulation competition, as influenced by the addition of phosphate or lime to soil.

In *E. coli*, the PHO regulon consists of some 30 genes in

eight operons whose expression is derepressed under phosphate-limiting conditions (43, 54). Transcription of these operons is regulated by the PhoB protein, which binds to similar 18-bp sequences (PHO boxes) in the regions of their promoters from positions -22 to -42. We have identified two tandem PHO-box-like sequences, located at bp -23 to -40 and -45 to -62 relative to the transcriptional start site of the *R. meliloti* *phoC* gene (Fig. 6). The *pstS* and *ugpB* promoters in *E. coli* have similarly arranged PHO boxes also, with a 4-nucleotide gap between boxes. As expression of the *phoD* and *phoE* genes is induced over 10-fold in response to phosphate starvation (Fig. 5), it is likely that the two putative PHO boxes in the *phoC* promoter are functional. It is also likely that *phoCDET*, and the other genes which constitute the PHO regulon in *R. meliloti*, will be derepressed under the low-phosphate conditions found in soil.

The recognition that the *phoCDET* genes encode a phosphate transport system is also of interest, as this locus is located on the 1,700-kb pEXO megaplasmid of *R. meliloti*. As in the case of genes involved in thiamine biosynthesis and carbohydrate utilization, and the other genes located on this plasmid (7, 16), the *phoCDET* genes are likely to be important to the life of the bacteria in the soil environment; however, they are clearly not essential for growth of the bacteria under all culture conditions.

#### ACKNOWLEDGMENTS

This work was supported by NSERC Research and Strategic grants to T.M.F.

We are grateful to Brian Golding and Dick and Brian Morton for advice and assistance with DNA and protein sequence analysis, Kim Napper for technical assistance, and Brian Driscoll and Ralf Voegele for critical comments on the manuscript.

#### REFERENCES

- Almendras, A. S., and P. J. Bottomley. 1987. Influence of lime and phosphate on nodulation of soil-grown *Trifolium subterraneum* L. by indigenous *Rhizobium trifolii*. *Appl. Environ. Microbiol.* **53**:2090-2097.
- Altschul, S. F., W. Gish, W. Miller, E. W. Myers, and D. J. Lipman. 1990. Basic local alignment search tool. *J. Mol. Biol.* **215**:403-410.
- Baichwal, V., D. Liu, and G. Ames. 1993. The ATP-binding component of a prokaryotic traffic ATPase is exposed to the periplasmic (external) surface. *Proc. Natl. Acad. Sci. USA* **90**:620-624.
- Bardin, S., and T. M. Finan. Unpublished data.
- Beck, D. P., and D. N. Munns. 1984. Phosphate nutrition of *Rhizobium* spp. *Appl. Environ. Microbiol.* **47**:278-282.
- Bielecki, R. L. 1973. Phosphate pools, phosphate transport, and phosphate availability. *Annu. Rev. Plant Physiol.* **24**:225-252.
- Charles, T. C., and T. M. Finan. 1991. Analysis of a 1600 kilobases *Rhizobium meliloti* megaplasmid using *in vivo* generated defined deletions. *Genetics* **127**:5-20.
- Charles, T. C., W. Newcomb, and T. M. Finan. 1991. NdvF, a novel locus located on megaplasmid pRmeSU47b (pExo) of *Rhizobium meliloti*, is required for normal nodule development. *J. Bacteriol.* **173**:3981-3992.
- Chen, C. M., Q.-Z. Ye, Z. Zhu, B. L. Wanner, and C. T. Walsh. 1990. Molecular biology of carbon-phosphorus bond cleavage. *J. Biol. Chem.* **265**:4461-4471.
- Claros, M. G., and G. von Heijne. 1994. TopPred II: an improved software for membrane protein structure predictions. *Comput. Appl. Biosci.* **10**:685-686.
- Dassa, E., and M. Hofnung. 1985. Sequence of gene *malG* in *E. coli*: homologues between integral membrane components from binding protein-dependent transport systems. *EMBO J.* **4**:2287-2293.
- Ditta, G. R., E. Viris, A. Palomares, and C. H. Kim. 1987. The *nifA* gene of *Rhizobium meliloti* is oxygen regulated. *J. Bacteriol.* **169**:3217-3223.
- Doige, C. A., and D. F.-L. Ames. 1993. ATP-dependent transport systems in bacteria and humans: relevance to cystic fibrosis and multidrug resistance. *Annu. Rev. Microbiol.* **47**:291-319.
- Dylan, T., P. Nagpul, D. R. Helinski, and G. R. Ditta. 1990. Symbiotic pseudorevertants of *Rhizobium meliloti* *ndv* mutants. *J. Bacteriol.* **172**:1409-1417.
- Finan, T. M., A. M. Hirsch, J. A. Leigh, E. Johansen, G. A. Kuldau, S. Deegan, G. C. Walker, and E. R. Signer. 1985. Symbiotic mutants of *Rhizobium meliloti* that uncouple plant from bacterial differentiation. *Cell* **40**:869-877.
- Finan, T. M., B. Kunkel, G. F. DeVos, and E. R. Signer. 1986. Second symbiotic megaplasmid of *Rhizobium meliloti* carrying exopolysaccharide and thiamine biosynthetic genes. *J. Bacteriol.* **167**:66-72.
- Fisher, H. M. 1994. Genetic regulation of nitrogen fixation in rhizobia. *Microbiol. Rev.* **58**:352-386.
- Froshauer, S., and J. Beckwith. 1984. The nucleotide sequence of the gene for the *malF* protein, an inner membrane component of the maltose transport system of *Escherichia coli*. *J. Biol. Chem.* **259**:10896-10903.
- Geremia, R. A., S. Cavaignac, A. Zorreguieta, N. Toro, J. Olivares, and R. A. Ugalde. 1987. A *Rhizobium meliloti* mutant that forms ineffective pseudonodules in alfalfa produces exopolysaccharides but fails to form  $\beta$ -(1-2) glucan. *J. Bacteriol.* **169**:880-884.
- Gribskov, M., J. Devereux, and R. R. Burgess. 1984. The codon preference plot: graphic analysis of protein coding sequences and prediction of gene expression. *Nucleic Acids Res.* **12**:539-548.
- Henikoff, S. 1984. Unidirectional digestion with exonuclease III creates targeted breakpoints for DNA sequencing. *Gene* **28**:351-359.
- Higgins, C. F. 1992. ABC transports: from microorganisms to man. *Annu. Rev. Cell Biol.* **8**:67-113.
- Higgins, D. G., A. J. Beasby, and R. Fuchs. 1992. CLUSTALV: improved software for multiple alignment. *Comput. Appl. Biosci.* **8**:189-191.
- Honeycutt, R. J., M. McClelland, and B. W. Sobral. 1993. Physical map of the genome of *Rhizobium meliloti* 1021. *J. Bacteriol.* **175**:6945-6952.
- Hynes, M., R. Simon, P. Muller, K. Niehaus, M. Labes, and A. Puhler. 1986. The two megaplasmids of *Rhizobium meliloti* are involved in the effective nodulation of alfalfa. *Mol. Gen. Genet.* **202**:356-362.
- Larson, T., G. Schumacher, and W. Boos. 1982. Identification of the *glpT*-encoded *sn*-glycerol-3-phosphate permease of *Escherichia coli*, an oligomeric integral membrane protein. *J. Bacteriol.* **152**:1008-1021.
- Lee, K., W. Metcalf, and B. Wanner. 1992. Evidence for two phosphonate degradative pathways in *Enterobacter aerogenes*. *J. Bacteriol.* **174**:2501-2510.
- Leigh, J. A., and D. L. Coplin. 1992. Exopolysaccharides in plant-bacterial interactions. *Annu. Rev. Microbiol.* **46**:307-346.
- Leigh, J. A., E. R. Signer, and G. C. Walker. 1985. Exopolysaccharide deficient mutants of *Rhizobium meliloti* that form ineffective nodules. *Proc. Natl. Acad. Sci. USA* **82**:6231-6234.
- Lerouge, P., P. Roche, C. Faucher, F. Maillet, G. Truchet, J. C. Prome, and J. Denaire. 1990. Symbiotic host specificity of *Rhizobium meliloti* is determined by a sulphated and acylated glucosamine oligosaccharide signal. *Nature (London)* **344**:781-784.
- Leung, K., and P. J. Bottomley. 1987. Influence of phosphate on the growth and nodulation characteristics of *Rhizobium trifolii*. *Appl. Environ. Microbiol.* **53**:2098-2105.
- Liu, C.-M., P. A. McLean, C. C. Sookdeo, and F. C. Cannon. 1991. Degradation of the herbicide glyphosate by members of the family *Rhizobiaceae*. *Appl. Environ. Microbiol.* **57**:1799-1804.
- Makino, K., M. Amemura, S. Kim, A. Nakata, and H. Shinagawa. 1994. Mechanism of transcriptional activation of the phosphate regulon in *Escherichia coli*, p. 5-12. In A. Torriani-Gorini, E. Yagil, and S. Silver (ed.), *Phosphate in microorganisms*, ASM Press, Washington, D.C.
- Makino, K., S. Kim, H. Shinagawa, M. Amemura, and A. Nakata. 1991. Molecular analysis of the cryptic and functional *phn* operons for phosphonate use in *Escherichia coli* K-12. *J. Bacteriol.* **173**:2665-2672.
- Manoil, C., and J. Beckwith. 1985. *tnpA*, a transposon probe for protein export signals. *Proc. Natl. Acad. Sci. USA* **82**:8129-8133.
- Metcalf, W. W., and B. L. Wanner. 1991. Involvement of the *Escherichia coli* *phn* (*psiD*) gene cluster in assimilation of phosphorus in the form of phosphonates, phosphite,  $P_i$  esters, and  $P_j$ . *J. Bacteriol.* **173**:587-600.
- Oliver, D. 1985. Protein secretion in *Escherichia coli*. *Annu. Rev. Microbiol.* **39**:615-648.
- Oresnik, I. J., T. C. Charles, and T. M. Finan. 1994. Second site mutations specifically suppress the Fix- phenotype of *Rhizobium meliloti* mutations on alfalfa: identification of a conditional *ndvF*-dependent mucoid colony phenotype. *Genetics* **136**:1233-1243.
- Osteras, M., B. T. Driscoll, and T. M. Finan. 1995. Molecular and expression analysis of the *Rhizobium meliloti* phosphoenolpyruvate carboxykinase (*pkcA*) gene. *J. Bacteriol.* **177**:1452-1460.
- Peters, N. K., J. W. Frost, and S. R. Long. 1986. A plant flavone, luteolin, induces expression of *Rhizobium meliloti* nodulation genes. *Science* **233**:977-980.
- Reed, J. W., and G. C. Walker. 1991. Acidic conditions permit effective nodulation of alfalfa by invasion-deficient *Rhizobium meliloti* *exoD* mutants. *Genes Dev.* **5**:2274-2287.
- Rosenberg, C., P. Boitard, J. Dénarié, and F. Casse-Delbart. 1981. Genes controlling early and late functions in symbiosis are located on a megaplasmid in *Rhizobium meliloti*. *Mol. Gen. Genet.* **184**:326-333.
- Rosenberg, H. 1987. Phosphate transport in prokaryotes, p. 205-248. In B. Rosen and S. Silver (ed.), *Ion transport in prokaryotes*. Academic Press, Inc., New York.
- Sambrook, J., E. F. Fritsch, and T. Maniatis. 1989. *Molecular cloning: a laboratory manual*, 2nd ed. Cold Spring Harbor Laboratory, Cold Spring Harbor, N.Y.

45. **Simon, R., J. Quandt, and W. Klipp.** 1989. New derivatives of transposon Tn5 suitable for mobilization of replicons, generation of operon fusions and introduction of genes in Gram-negative bacteria. *Gene* **80**:161–169.
46. **Smart, J. B., M. J. Dilworth, and A. D. Robson.** 1984. Effect of phosphorus supply on phosphate uptake and alkaline phosphatase activity in Rhizobia. *Arch. Microbiol.* **140**:218–286.
47. **Smart, J. B., A. D. Dobson, and M. J. Dilworth.** 1984. A continuous culture study of the phosphorus nutrition of *Rhizobium trifolii* WU95, *Rhizobium* NGR234 and *Bradyrhizobium* CB756. *Arch. Microbiol.* **140**:276–280.
48. **Soupène, E., M. Foussard, P. Boistard, G. Truchet, and J. Batut.** 1995. Oxygen as a key developmental regulator of *Rhizobium meliloti* N<sub>2</sub>-fixation gene expression within the alfalfa root nodule. *Proc. Natl. Acad. Sci. USA* **92**:3759–3763.
49. **Spaink, H. P., D. M. Sheeley, A. A. van Brussel, J. Glushka, W. S. York, T. Tak, O. Geiger, E. P. Kennedy, V. N. Reinhold, and B. J. Lugtenberg.** 1991. A novel highly unsaturated fatty acid moiety of lipo-oligosaccharide signals determines host specificity of *Rhizobium*. *Nature (London)* **354**:125–130.
50. **van Veen, H. W., T. Abee, G. J. J. Kortstee, W. N. Konings, and A. J. B. Zehnder.** 1993. Mechanism and energetics of the secondary phosphate transport system of *Acinetobacter johnsoni* 210A. *J. Biol. Chem.* **268**:19377–19383.
51. **van Veen, H. W., T. Abee, G. J. J. Kortstee, W. N. Konings, and A. J. B. Zehnder.** 1994. Substrate specificity of the two phosphate transport systems of *Acinetobacter johnsoni* 210A in relation to phosphate speciation in its aquatic environment. *J. Biol. Chem.* **269**:16212–16216.
52. **Vieirra, J., and J. Messing.** 1987. Production of single-stranded plasmid DNA. *Methods Enzymol.* **153**:3–34.
53. **von Heijne, G.** 1986. The distribution of positively charged residues in bacterial inner membrane proteins correlates with the trans-membrane topology. *EMBO J.* **5**:3021–3027.
54. **Wanner, B. L.** 1993. Gene regulation by phosphate in enteric bacteria. *J. Cell. Biochem.* **51**:47–54.
55. **Winans, S.** 1990. Transcriptional induction of an *Agrobacterium* regulatory gene at tandem promoters by plant-released phenolic compounds, phosphate starvation, and acidic growth media. *J. Bacteriol.* **172**:2433–2438.
56. **Yarosh, O. K., T. C. Charles, and T. M. Finan.** 1989. Analysis of C4-dicarboxylate transport genes in *Rhizobium meliloti*. *Mol. Microbiol.* **3**:813–823.